Metallophysics and Advanced Technologies
Металофіз. новітні технол.
Metallofiz. Noveishie Tekhnol.
2022, vol. 44, No. 5, pp. 601–611
https://doi.org/10.15407/mfint.44.05.0601
Reprints available directly from the publisher

PACS numbers: 45.50.-j, 47.10.ab, 47.27.nd, 47.40.Ki, 52.77.Fv, 81.15.-z

Simulation of Gas Flow with Nanocomposite Carbon-Containing Powders in Supersonic Nozzle

O. V. Shorinov and S. A. Polyviany*

National Aerospace University 'Kharkiv Aviation Institute',
17 Chkalov Str.,
UA-61070 Kharkiv, Ukraine
**Motor Sich JSC,*
15 Motorostroiteley Ave.,
UA-69068 Zaporizhzhya, Ukraine

Modern technologies for producing carbon nanostructures are based on many years of experience in the development of coating methods. The latest trends in the formation of carbon nanostructures are associated with complex technological processes of physical and technical treatment, when microstructures are obtained based on traditional methods, which are then completely or partially modified into nanostructures. In this case, the possibility of the formation of a part of nanostructures in a gas flow is considered in order to use them as islands of growth of other nanostructures on the treated surface. The conditions for formation of the specified structures are characterized by the energy state of particles, physical and mechanical properties of particles and substrate materials. The paper presents the results of numerical simulation for determination of velocity and temperature of nanocomposite metal-matrix powder particles in a supersonic nozzle. The necessity to determine parameters of solid particles of powder in a two-phase supersonic flow is determined. Particles velocity and temperature are the crucial parameters which allow for formation of coatings and impact their physical and mechanical properties. The contour plots of velocity and temperature distribution in the nozzle and free space from the nozzle exit to the substrate are obtained. Coating application and its characteristics are considered when selecting coating materials. The numerical simulation is performed for the particles of boron carbide (B_4C) and nickel (Ni) powders. The dependence of velocity and

Corresponding author: Oleksandr Volodymyrovych Shorinov
E-mail: o.shorinov@khai.edu

Citation: O. V. Shorinov and S. A. Polyviany, Simulation of Gas Flow with Nanocomposite Carbon-Containing Powders in a Supersonic Nozzle, *Metallofiz. Noveishie Tekhnol.*, **44**, No. 5: 601–611 (2022). DOI: 10.15407/mfint.44.05.0601

temperature of nano-sized B_4C particles in the nozzle on the gas initial conditions is analysed. The obtained results are an important stage in the development of optimal technological processes of coating deposition with selection of a rational ratio between velocity and temperature of the sprayed particles.

Key words: nanocomposite coatings, supersonic nozzle, cold spraying, micro- and nanopowders, two-phase flow.

Сучасні технології одержання вуглецевих наноструктур спираються на багаторічний досвід розвитку метод нанесення покриттів. Останні тенденції в області формування вуглецевих наноструктур пов'язані з комплексними технологічними процесами фізико-технічного оброблення, коли на основі традиційних метод одержують мікроструктури, які потім повністю або частково модифікуються в наноструктури. При цьому розглядається можливість утворення частини наноструктур в газовому потоці, з тим, щоб використовувати їх в якості острівців зростання інших наноструктур на оброблюваній поверхні. Умовами формування певних структур є енергетичний стан частинок, фізико-механічні властивості матеріялів частинок та підложжя. У роботі представлено результати комп'ютерного моделювання із визначення швидкости та температури частинок нанокомпозитних метало-матричних порошків у надзвуковому соплі. Сформульовано проблему необхідности визначення параметрів твердої частини порошку в двофазному надзвуковому потоці. Швидкість і температура частинок порошку є найважливішими параметрами, від яких залежить можливість формування покриття, а також їх фізико-механічні характеристики. Одержано поля розподілу швидкости та температури потоку в соплі та вільному просторі від зрізу сопла до підложжя. При виборі порошкових матеріялів для дослідження було враховано службове призначення покриттів та їх властивості. У даній роботі моделювання проведено для частинок порошку карбіда Бору B_4C та Ніклю Ni. Встановлено залежність швидкости та температури нанорозмірних частинок B_4C в каналі сопла від параметрів газового потоку на вході нього. Одержані результати є важливим етапом розроблення оптимальних технологічних процесів напилювання з вибором раціонального співвідношення між швидкістю та температурою частинок, що напилюються.

Ключові слова: нанокомпозитні покриття, надзвукове сопло, холодне напилювання, мікро- і нанопорошки, двофазний потік.

(Received December 10, 2020; in final version, November 5, 2021)

1. INTRODUCTION

Carbon nanomaterials are considered as promising candidates for large number of applications such as for FETs [1], supercapacitors [2], nanofluid applications [3], photovoltaic devices [4] and field emitters [5]. Metal-matrix composite carbon-containing coatings can be applied in order to increase surface properties of the parts. These coatings consist of a mixture of metal and carbides or oxides powders. Currently,

the following methods are used to obtain such coatings: laser cladding [6], plasma spraying [7] and deposition [8], and electron-beam cladding [9], to mention a few. Various technologies are applied to treat the surface to grow the nanostructures [10, 11], and most of them are grounded on the physical effects occurring at the interaction of the gas-phase [12], plasma [13] or sprayed material [14] with a treated substrate. Among them, the technology of cold gas-dynamic spraying is a promising method for applying nanocomposite coatings [15].

Cold spraying (CS) is a coating method based on the effect of formation of a strong metal layer during interaction of two-phase (gas + solid particles) supersonic flow with a substrate. The principal difference from the well-known gas-thermal methods (plasma, detonation, gas-flame, *etc.*) is that the main energy source in the coating processes is the kinetic energy of not relatively light-weighted ions, atoms, or molecules [16], but of heavy high-velocity solid particles, which are the clusters of the material. The physical mechanism of CS coating is a high-velocity deformation of particles on impact, which causes intensive shear instability of the material along the contact boundaries and formation of adhesive-cohesive bonds [17].

Metal-matrix composite coatings based on boron carbide (B_4C) and nickel (Ni) metal base are of particular interest. Utilization of B_4C with its unique properties (high hardness, low density, *etc.*) in the initial mixture can significantly improve physical and mechanical properties of composite coating. The selection of nickel as a metal base is due to its satisfactory machining and good corrosion resistance properties.

In recent years, deposition of nanocomposite coatings by cold spraying has become an urgent problem. V. M. Fomin *et al.* [18] have suggested a novel method of formation of heterogeneous $Ni + B_4C$ coating based on cold spray deposition process with subsequent laser treatment.

Paper [19] shows the study results of titanium-based coating properties with addition of silicon carbide and boron carbide particles. The obtained coatings have showed low porosity ($< 1\%$). The coatings microhardness amounted to $98 \pm 29\ HV_{-0,1}$, $139 \pm 65\ HV_{-0,1}$ and $258 \pm 115\ HV_{-0,1}$ for Ti, $Ti + B_4C$ and $Ti + SiC$ compositions, respectively.

Influence of hard particles content on microhardness and thickness of $Al + B_4C$, $Cu + B_4C$, $Ti + B_4C$ and $Ni + B_4C$ coatings was investigated in [20]. It was found that adding of B_4C to the powder composition leads to increase of microhardness of composite coatings by comparison with microhardness of studied metal coatings without carbide solid particles. It was showed that an increase of B_4C volume concentration in a powder mixture leads to decrease of coating thickness. The coatings porosity was less than 2%.

A numerical simulation of two-phase flow in low-pressure cold

spraying supersonic nozzle is described in enough detail in [21–23]. However, an analysis of current state of the art in a field of cold spraying showed that previous studies were aimed at experimental research of the spraying process of nanocomposite powder composition and it lacks information of theoretical investigation of the process.

The development of mathematical models for prediction of particles parameters in a gas flow is an important stage in optimization process of cold spraying and development of technological recommendations. The aim of this study is to determine the energy parameters of particles of nanocomposite coatings in low-pressure cold spraying supersonic nozzle in order to develop spraying technologies and new equipment.

2. SIMULATION DETAILS

2.1. Calculation Model, Boundary and Initial Conditions

The ANSYS FLUENT software was used for flow simulation. The calculation was conducted for standard low-pressure cold spraying nozzle SK-20 (Fig. 1).

The initial conditions for the simulation were: nozzle geometry, parameters of the flow at the nozzle inlet and properties of powder particles. Boundary and initial conditions were used to set the pressure and temperature of the working gas at the nozzle inlet, axis of symmetry, walls, ambient temperature and pressure.

The substrate was tagged as a wall at a distance of 15 mm from the nozzle outlet. Air was used as the working gas. Air pressure at the nozzle inlet was set at 1.0 MPa. The inlet air temperature was set in the range from 573 to 873 K. The simulation was performed for B_4C and Ni powders with a particle size of 500 nm and 15 μm respectively. The powder was fed perpendicular to the axis of the nozzle through the powder supply channel named as Powder Inlet (Fig. 1). The powder particles velocity at the Powder Inlet was set at 20 m/s with the temperature of 300 K. Acceleration of the air-powder mixture to the supersonic velocity was observed in the divergent part of the nozzle, consisting of four consecutive cylindrical sections (Fig. 1). The ambient

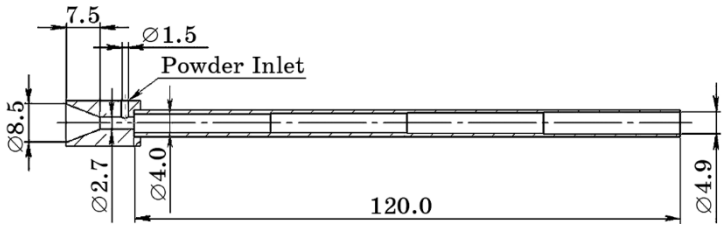

Fig. 1. SK-20 nozzle geometry.

pressure and temperature were 1 bar and 300 K respectively. The calculation model with boundary conditions is schematically shown in Fig. 2.

In order to obtain the optimal size of the calculated mesh, a series of preliminary simulations were performed. It was found that reducing the mesh size less than 0.2×0.2 mm does not increase the accuracy of calculations, but increases the calculation time.

2.2. The Governing Equations of Turbulent Flow

The gas flow in cold spraying is compressible, viscous and turbulent. The model which is used in simulation is based on the Navier–Stokes system of differential equations with the Reynolds method of averaging the time-dependent equations together with the standard k–ε turbulence model. Governing equations for turbulent flow are the following [24]:

1) Conservation of mass:

$$\frac{d}{dx_j}(\rho_g V_j) = 0, \tag{1}$$

where ρ_g is the gas density, V_j is the velocity vector in the j^{th} direction;

2) Conservation of momentum:

$$\frac{d}{dx_j}(\rho_g V_i V_j) = -\frac{dp}{dx_i} + \frac{d\tau_{ij}}{dx_i} + \rho_g g_i, \tag{2}$$

where τ_{ij} is the stress, g_i is the gravitational acceleration.

The stress can be given by

$$\tau_{ij} = \left[(\mu + \mu_t)\left(\frac{dV_i}{dx_j} + \frac{dV_j}{dx_i}\right)\right] - \frac{2}{3}\mu_t \frac{dV_j}{dx_i}\delta_{ij}, \tag{3}$$

where μ is the molecular viscosity, $\delta_{ij} = 1$ for $i = j$, otherwise $\delta_{ij} = 0$, μ_t is turbulent viscosity given by

$$\mu_t = \rho_g C_\mu \frac{k_t^2}{\varepsilon_t}, \tag{4}$$

where C_μ is the constant, $C_\mu = 0.09$, k_t is the kinetic energy of turbulence, ε_t is the dissipation of kinetic energy of turbulence, which can be defined in the k–ε turbulence model.

A standard k–ε model of turbulence is usually used to close the system of equations (1)–(4). In accordance with FLUENT User Guide [25], these are

$$\frac{d}{dx_i}(\rho_g V_i k) = \frac{d}{dx_i}\left(\frac{\mu_t}{\sigma_k}\frac{dk}{dx_i}\right) + G_k + G_b - \rho_g \varepsilon_t, \tag{5}$$

$$\frac{d}{dx_i}(\rho_g V_i \varepsilon_t) = \frac{d}{dx_i}\left(\frac{\mu_t}{\sigma_\varepsilon}\frac{d\varepsilon_t}{dx_i}\right) + G_{1\varepsilon}\frac{\varepsilon_t}{k_t}(G_k + G_b) - G_{2\varepsilon}\rho_g \frac{\varepsilon_t^2}{k_t}, \tag{6}$$

where $C_{1\varepsilon}$, $C_{2\varepsilon}$, σ_k, σ_ε are the empirical constants, σ_h is the turbulent Prandtl number, $\sigma_h = \mu_t C_p / kt$, G_k is the rate of production of kinetic energy of turbulence:

$$G_k = \mu_t\left(\frac{dV_j}{dx_i} + \frac{dV_i}{dx_j}\right)\frac{dV_i}{dx_j}, \tag{7}$$

G_b is the generation of turbulence due to buoyancy:

$$G_b = -g_t \frac{\eta_t}{\rho_g \sigma_h}\frac{d\rho_g}{dx_i}. \tag{8}$$

The presence of a solid dispersed phase in a two-phase flow can be described using the second transport equation. The trajectory of the particle of the dispersed phase is determined by the integration of the balance of forces acting on the particle in the Lagrangian coordinate system (Lagrange method for tracking the trajectory of the particle) [26].

In order to simplify the calculations, some assumptions are made: the shape of a particle is spherical, the particle is solid and inert. Calculations are performed for the single particle in the gas flow. The interaction between the particles is neglected because the volume concentration of particles is quite small [27]. Also, the calculations do not consider the force of gravity, because the residence time of the particle in the flow is very small.

The force balance equation acting on a particle can be written in the following form [28]:

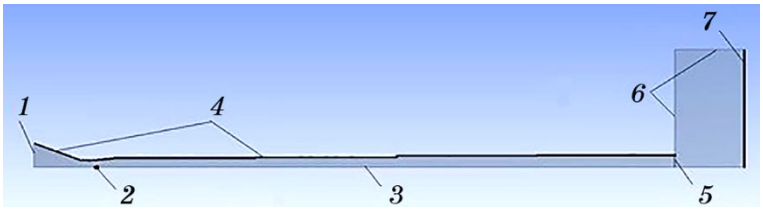

Fig. 2. Boundary conditions for the simulation: *1*—nozzle inlet, *2*—particle inlet, *3*—nozzle axis, *4*—nozzle walls, *5*—nozzle outlet, *6*—non-reflective boundaries, *7*—substrate.

$$\frac{dV_{\mathrm{p},i}}{dr} = f_{\mathrm{D}}(V_{\infty.i} - V_{\mathrm{p},i}) + \frac{g_i(\rho_{\mathrm{p}} - \rho_{\infty})}{\rho_{\mathrm{p}}} + F_i, \tag{9}$$

where $f_{\mathrm{D}}(V_{\infty.i} - V_{\mathrm{p},i})$ is the drag force per unit mass of the particle:

$$f_{\mathrm{D}} = \frac{18\mu}{\rho_{\mathrm{p}} d_{\mathrm{p}}^2} \frac{C_{\mathrm{D}} Re}{24}, \tag{10}$$

where Re is the relative Reynolds number, which is defined as

$$Re = \frac{\rho_{\infty} d_{\mathrm{p}} \left| V_{\mathrm{p},i} - V_{\infty,i} \right|}{\mu}, \tag{11}$$

C_{D} is the drag coefficient and is a function of the relative Reynolds number

$$C_{\mathrm{D}} = \alpha_1 + \frac{\alpha_2}{Re} + \frac{\alpha_3}{Re^2}, \tag{12}$$

where α_1, α_2, α_3 are the constants that apply over several ranges of Re.

The velocity of the particle at each point along the trajectory can be predicted by integration of equation (9) with (12)

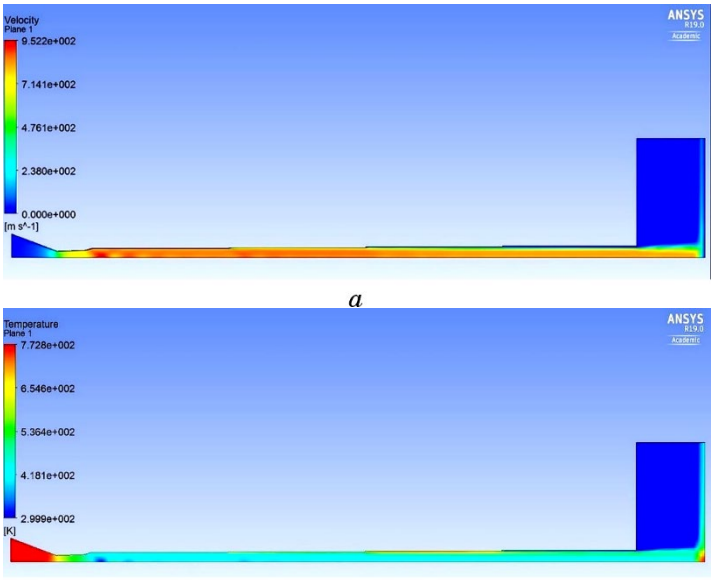

a

b

Fig. 3. Gas flow simulation results at $P_0 = 1.0$ MPa and $T_0 = 723$ K: gas velocity (*a*), gas temperature (*b*).

$$\frac{dx_i}{dr} = V_{\mathrm{p},i}. \tag{13}$$

3. RESULTS AND DISCUSSION

Figure 3 shows simulation results for gas velocity (*a*) and temperature (*b*) at the following gas inlet parameters: temperature is 723 K and pressure is 1.0 MPa.

The results show that the acceleration of the gas occurs in the nozzle throat and at the beginning of divergent part of the nozzle. Gas temperature in the convergent part of the nozzle decreases to about 80% of its initial temperature at the nozzle inlet. Further decrease in gas temperature in the divergent part of the nozzle depends on the nozzle expansion ratio.

Figures 4 and 5 show simulation results of velocities and temperatures of B_4C and Ni particles depending on the gas temperature at the nozzle inlet.

As can be seen from the results of the simulation, an increase in gas inlet temperature leads to increase of gas velocity and temperature which can be explained by the following equation:

$$V = \sqrt{\gamma RT}, \tag{14}$$

where R is specific gas constant, γ is gas molecular weight, T is gas temperature.

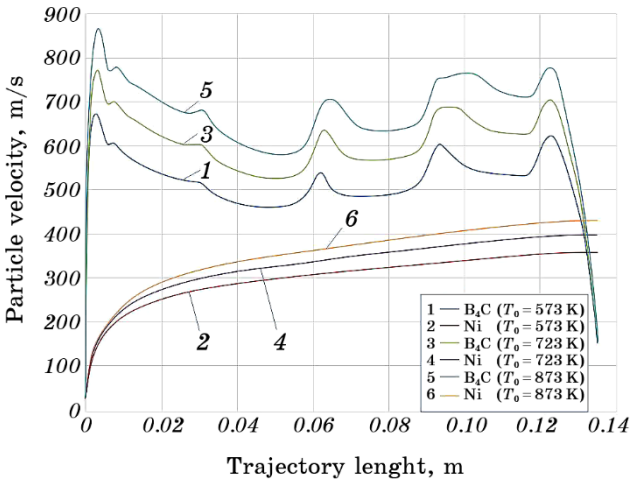

Fig. 4. B_4C and Ni particle velocity at different nozzle inlet gas temperature T_0.

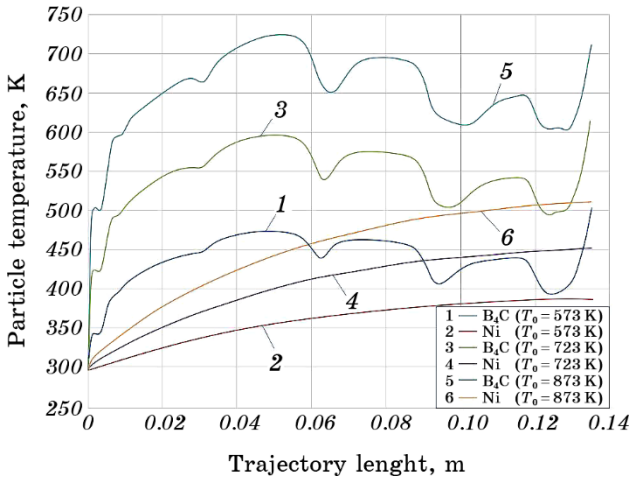

Fig. 5. B_4C and Ni particle temperature at different nozzle inlet gas temperature T_0.

Result demonstrates that inlet gas temperature affects the temperature and velocity of particles. An increase in gas velocity leads to increase of velocity of particles in this flow. An increase in temperature from 573 K to 873 K leads to an increase in the impact velocity of B_4C particle from 145.6 m/s to 168.9 m/s and the particle impact temperature from 502.6 K to 710.5 K at a constant pressure of 1 MPa and the spraying distance of 15 mm. For 15 mm nickel particles at the same spraying parameters, the particle impact velocity increases from 357.6 m/s to 429.6 m/s and the particle impact temperature increases from 388.2 K to 512 K. A sharp drop of the impact velocity of B_4C particles can be explained with bow-shock development on the substrate surface. The bow-shock leads to deceleration of nano-sized particles and, to a lesser degree effects on micro-sized Ni particles.

4. CONCLUSION

Simulation of two-phase flow in a low-pressure cold spraying supersonic nozzle was carried out. The temperature and velocity for nano-sized particles of B_4C powder were obtained depending on the gas temperature at the nozzle inlet. The results were compared with the results of micro sized particles of Ni powder at the same spraying condition. Obtained results are important for further studying of cold spraying process, modification, and development of spraying equipment in order to develop a novel functionally gradient nanocomposite coating.

The authors would like to acknowledge financing of National Re-

search Foundation of Ukraine under grant agreement No. 190/02.2020.

REFERENCES

1. M. M. Shulaker, J. Van Rethy, G. Hills, H. Wei, H.-Y. Chen, G. Gielen, H.-S. Philip Wong, and S. Mitra, *IEEE J. Solid-St. Circ.*, **49**, No. 1: 190 (2014).
2. J. Li, X. Cheng, A. Shashurin, and M. Keidar, *Graphene*, **1**, No. 1: 1 (2012).
3. U. Legrand, N.-Y. M. Gonzalez, P. Pascone, J.-L. Meunier, and D. Berk, *Carbon*, **102**: 216 (2016).
4. L. Shi, C. Pang, S. Chen, M. Wang, K. Wang, Z. Tan, P. Gao, J. Ren, Y. Huang, H. Peng, and Z. Liu, *Nano Lett.*, **17**, No. 6: 3681 (2017).
5. M. Y. Zhu, R. A. Outlaw, M. Bagge-Hansen, H. J. Chen, and D. M. Manos, *Carbon*, **49**, No. 7: 2526 (2011).
6. Q. W. Meng, T. L. Geng, and B. Y. Zhang, *Surf. Coat. Tech.*, **200**: 4923 (2006).
7. H. Zhu, Y. Niu, C. Lin, L. Huang, H. Ji, and X. Zheng, *Ceram. Int.*, **39**: 101 (2013).
8. O. Baranov, J. Fang, A. Rider, S. Kumar, and K. Ostrikov, *IEEE Transactions Plasma Sci.*, **41**, No. 12: 3640 (2013).
9. D. Mul, D. Krivezhenko, T. Zimoglyadova, A. Popelyukh, D. Lazurenko, and L. Shevtsova, *Appl. Mech. Materials*, **788**: 241 (2015).
10. O. Baranov, M. Romanov, M. Wolter, S. Kumar, X. Zhong, and K. Ostrikov, *Phys. Plasmas*, **17**: 053509 (2010).
11. K. Bazaka, I. Levchenko, J. W. M. Lim, O. Baranov, C. Corbella, S. Xu, and M. Keidar, *J. Phys. D Appl. Phys.*, **52**: 183001 (2019).
12. C. Ma, P. Hou, X. Wang, Z. Wang, W. Li, and P. Kang, *Appl. Catal. B-Environ.*, **250**, No. 5: 347 (2019).
13. I. Levchenko, M. Romanov, O. Baranov, and M. Keidar, *Vacuum*, **72**: 335 (2004).
14. H. Wang, P. He, G. Ma, B. Xu, Z. Xing, S. Chen, Z. Liu, and Y. Wang, *J. Eur. Ceram. Soc.*, **38**, No. 10: 3660 (2018).
15. R. N. Raoelison, C. Verdy, and H. Liao, *Mater. Design*, **133**: 266 (2017).
16. O. Baranov and M. Romanov, *Plasma Process Polym.*, **5**: 256 (2008).
17. A. P. Alkhimov, V. F. Kosarev, and A. N. Papyrin, *J. Appl. Mech. Tech. Phys.*, **39**, No. 2: 318 (1998).
18. V. M. Fomin, A. A. Golyshev, V. F. Kosarev, A. G. Malikov, A. M. Orishich, N. S. Ryashin, A. A. Filippov, and V. S. Shikalov, *Prikladnaya Mekhanika i Tekhnicheskaya Fizika*, **58**, No. 5: 218 (2017) (in Russian).
19. N. S. Ryashin, V. S. Shikalov, I. S. Batraev, V. F. Kosarev, S. V. Klinkov, V. M. Fomin, and N. V. Mironov, *AIP Conference Proceedings*, **2027**: 030096 (2018).
20. T. M. Vidyuk, V. F. Kosarev, S. V. Klinkov, and V. S. Shikalov, *AIP Conference Proceedings*, **2125**: 030025 (2019).
21. A. I. Dolmatov, S. V. Sergeev, M. A. Kurin, V. V. Voron'ko, and T. V. Loza, *Metallofiz. Noveishie Tekhnol.*, **37**, No. 7: 871 (2015) (in Russian).
22. A. I. Dolmatov and A. V. Bil'chuk, *Metallofiz. Noveishie Tekhnol.*, **40**, No. 9: 1257 (2018) (in Russian).
23. A. I. Dolmatov and A. V. Bil'chuk, *Metallofiz. Noveishie Tekhnol.*, **41**, No. 7:

927 (2019) (in Russian).
24. N. Rajaratnam, *Turbulent Jets* (Amsterdam: Elsevier: 1976).
25. *FLUENT. 4.4.4 User Guide* (Munich: Fluent Inc., SimScale: 1996).
26. A. I. Dolmatov, K. A. Danko, and Y. O. Neveshkin, *Metallofiz. Noveishie Tekhnol.*, **36**, No. 11: 1533 (2014).
27. T. Stoltenhoff, H. Kreye, and H. J. Richter, *J. Therm. Spray Techn.*, **11**, No. 4: 542 (2002).
28. D. Gidaspow, *Multiphase Flow and Fluidization: Continuum and Kinetic Theory Descriptions* (New York: Academic Press: 1994).